iJRASET
International Journal For Research in Applied Science and Engineering Technology



INTERNATIONAL JOURNAL FOR RESEARCH

IN APPLIED SCIENCE & ENGINEERING TECHNOLOGY

Volume: 14 **Issue:** III **Month of publication:** March 2026

DOI: https://doi.org/10.22214/ijraset.2026.78834

www.ijraset.com

Call: 08813907089 | E-mail ID: ijraset@gmail.com

International Journal for Research in Applied Science & Engineering Technology (IJRASET)
ISSN: 2321-9653; IC Value: 45.98; SJ Impact Factor: 7.538
Volume 14 Issue III Mar 2026- Available at www.ijraset.com

Synthesis and Characterization of $Ba_{0.5}Sr_{0.5}(Co_{0.8}Fe_{0.2})_{1-x}Zr_xO_{3-\delta}$(BSCFZ)Cathode for Solid Oxide Fuel Cell

Mr.D.Rama Krishna Sharma[1], Dr.P.Vijay Bhaskar Rao[2]
[1]*Department of Physics, Jawaharlal Nehru Technological University, Hyderabad*
[2]*Professor and Director, R&D, St. Mary Engineering College, Deshmukhi, Hyderabad, India*

Abstract: ***The BSCFZ, Barium Strontium Cobalt Iron Zirconate{Ba0.5Sr0.5(CO0.8 Fe0.2)1-xZ r xO3-δ} [Where δ is the deficiency of oxygen and x = 0, 0.10, 0.15, 0.20)], powders have been synthesized by sol-gel process using nitrate based powdered chemicals for SOFC applications as these powders are more useful for cathodes and anodes for SOFCs since these powders are considered to be more promising cathode materials for SOFC.Ionic conduction, Adsorption and desorption rates are the major processes that control the electrode reactions. They contribute to theoverpotential. To obtain thelow potential cathodematerials suitable for electrolytes, Sol-Gel methodisusedandnanopowdersareprepared.Thechelatingagentusedis Aceticacid,Ethylene glycol & Ammoniaasdispersant.Thesepowderswerekept forcalcinationsat 900^{0}C for16hours andat 1050^{0}Cforabout 6hoursincruciblesofhighaluminain furnace. Thesewerecharacterized by XRD; SEM with EDAX, Densities, TGA, DTA, FTIR and conductivities.XRD results proved the formation of Perovskite phase at all calcination temperatures. From SEM, it is found that for some samples, there is presence of extreme porous particlesin nano sizes and conductivities, densities are studied.***
Keywords: DENSITY, XRD, SEM, SEM/EDAX,TGA/DTA, IMPEDANCE {Ba0.5Sr0.5(Co0.8Fe0.2)1-xZrxO3-δ}

I. INTRODUCTION

Recently strontium doped cobaltitehas attracted much attention because of its mixed conduction characteristics and its relatively high ionic conductivity. Strontium doped samarium cobaltite (SmSrCoO: SSC) shows even higher conductivity, up to 10Scm [13]. It shows good compatibility with ceria cathode. The cathodic reaction mechanism ofSSC is not clearly understood. Ionic conduction, Adsorption and desorption rates are known as the major processes that control the electrode reactions. They contribute to the over potential In practical the adsorption and desorption rates of SOFC are not equal. Therefore separate adsorption and desorption rates must be determined.ZhaoyuZhonget.al.(https://doi.org/10.1016/j.ceramint.2023.11.113)studiedtheHigh-performance $BaZr_{0.1}Ce_{0.7}Y_{0.1}Yb_{0.1}O_{3-\delta}$ (BZCYYb) protonic ceramic fuel cell electrolytes by the Ba evaporation inhibition strategy. Their results showed that Ba evaporation inhibition strategyis proven to be an effective method to fabricate stoichiometric BZCYYb electrolytes. Thecontent of A-site cation, Ba is strongly related to the chemical composition, grain size and electrochemical properties of the electrolyte. The main conclusions are as follows: The relative atomic ratio of Ba is normalized. B-BZCYYb shows a Ba/(Zr + Ce + Y + Yb) of 0.97 ± 0.09, whilethevalueofA-BZCYYbisonly0.63±0.06.Outofvariousfuelcells,solid-oxidefuel cells (SOFCs) have the benefit of eco-friendly power generation with fuel [15] flexibility. High operatingtemperaturesresultedinhighlyexpensive,lesscompactnessandlowcompatibility.

Hencebyenhancingtheporosityofcathode;onecanincreasetheoxygenexchangeanddiffusion in cathode which results to higher current density in the cell. Since six years $Ba_{0.5}Sr_{0.5}[Co_{0.8}Fe_{0.2}]_{1-x}Zr_xO_{3-\delta}$and other combinations have got much attention for intermediate temperature of SOFCs but, this reduction in operating temperature below 800^{o}C causes an increase of the over potential ofSOFC cathode. Therefore, to obtain the low potential cathode materials, the material$Ba_{0.5}Sr_{0.5}[Co_{0.8}Fe_{0.2}]_{1-x}Zr_xO_{3-\delta}$is designed, {where 'x' isVarious Compositions and 'δ' is deficiency of oxygen(0, 0.1,0.15 and 0.20)}.Bytakingsuch dopingofZirconiumwithBSCF,theweight %wasfound tobein the present paper, the objective of the author is to prepare a cathode suitable for SOFC in single chamber fuel cell conditions. Hence, materials with a small percentage of Zr (with increasing values), BSCF samples are prepared by sol-gel method and their characterization/values are compared.

©IJRASET: All Rights are Reserved

International Journal for Research in Applied Science & Engineering Technology (IJRASET)
ISSN: 2321-9653; IC Value: 45.98; SJ Impact Factor: 7.538
Volume 14 Issue III Mar 2026- Available at www.ijraset.com

II. EXPERIMENTAL

A. *Materials:*

Commercial powders of AR grade of Aldrich Company were used in this work for the preparation of Cathode. Ethylene di-amine-tetra-acetic acid (EDTA), ethylene glycol, anhydrous citric acid, nitrate salts of Barium, Strontium, Cobalt, Iron and Zirconium oxide were purchased from Sigma Aldrich, USA. Ammonia solution is used as base. In the present observations, the Nano crystalline cathode material of **$Ba0.5Sr0.5[Co0.8Fe0.2]_{(1-x)}Zr_xO3-\delta$** by varying x values, (x = 0, 0.10, 0.15, 0.20) BSCF Zr (5582TZr powders were prepared by sol-gel process as it is one of the economical ways and characterizations like SEM/ EDAX of LEO SUPRA 55 VD ultra-high resolution of ZEISS, XRD TGA/DTA, Raman spectroscopy Impedance Analyzer were used. Barium nitrate Ba $(NO3)_2$,StrontiumNitrateSr$(NO3)_2$,CobaltousNitrateCo $(NO3)_2$, FlukaFe$(NO_3)_2.9H_2O$ &ZrO_2, are used.

Flowchart of Experiment:

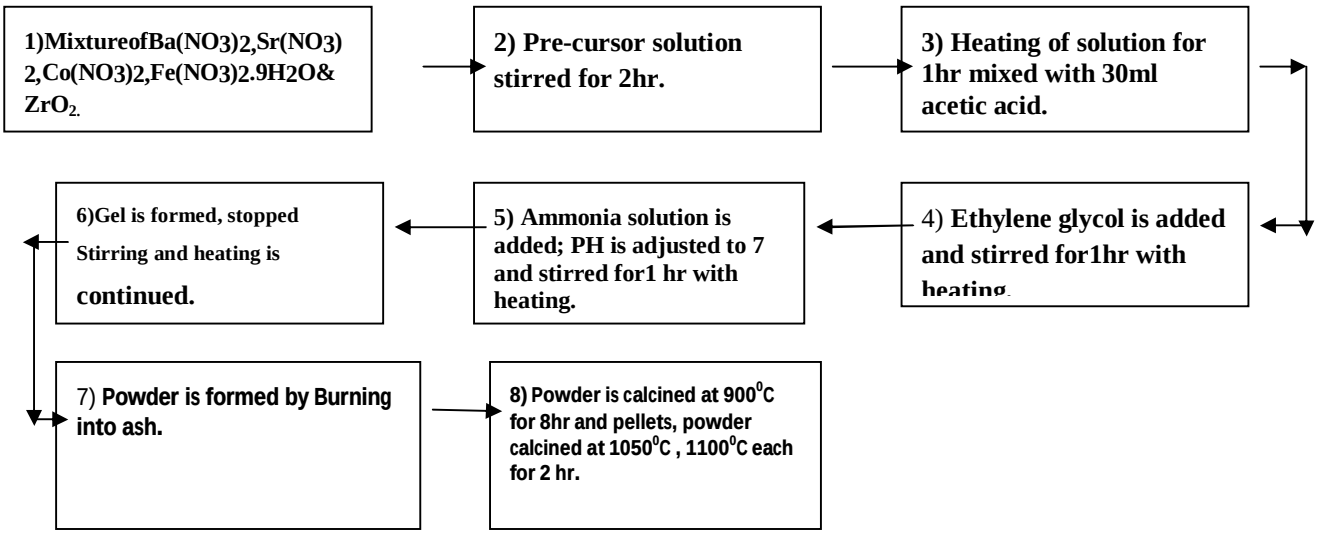


Figure: 1

B. *Method:*

Precursorsolutionispreparedbytakingabovepowdersbyappropriateformulaandmixingaqueous solution of the above chemicals in molar ratio of 0.5:0.5 and 0.8:0.2 & required Acetic acid, ammonia, are added and ratio is maintained as 0.5. The solution is taken in borosil glass beaker and placed on a Magnetic stirrer with hot plate for about 4 hr with appropriate speed and by heating at about 80^0C to 100^0C, the solution is stirred till it becomes like a gel and then, the speed is reduced, heated for some time till it becomes ash after burning. The ash is calcined first at 750^0C, for8 hr, and at 900^0C, for8 hrand at 1050^0C, 1100^0C each for2 hrand after preparing pellets, their densities are calculated as in table.1

S.No.	Sample	Wt. in air (g)	Wt.in Xylene(g)	ρ_{exp} = Wt.in air/Loss of wt. in Xylene	a(Lattice constant) Å	ρ_{th}=nM/a^3N_A (g/cc)	Density% = {ρexp/ρth}*100
1.	Zr_1	0.5350	0.4408	4.9161	3.99970	5.063	97
2.	Zr_2	0.7266	0.5975	4.9042	4.16309	5.038	97.3
3.	Zr_3	0.5954	0.4912	4.9506	4.17023	5.050	98
4.	Zr_4	0.5552	0.4587	4.9749	4.19864	5.093	97.6

Table.1Densitycalculations.

Sample	Cathode powder	c/n
Zr_1	Ba0.5Sr0.5[Co0.8Fe0.2] O2	0.5
Zr_2	Ba0.5Sr0.5[Co0.8Fe0.2]0.9Zr0.1 O2	0.5
Zr_3	Ba0.5Sr0.5[Co0.8Fe0.2]0.85Zr0.15 O2	0.5
Zr_4	Ba0.5Sr0.5[Co0.8Fe0.2]0.8Zr0.20 O2	0.5

Table2.CathodeBSCFZr–5582Zr)powdersbysol-gelprocess.

©IJRASET: All Rights are Reserved

ISSN: 2321-9653; IC Value: 45.98; SJ Impact Factor: 7.538
Volume 14 Issue III Mar 2026- Available at www.ijraset.com

III. CHARACTERIZATION

A. XRD Characterization:

X-ray diffraction (XRD) analysis of the sintered samples is carried out with XRD at 40 KV and 30mA,usingCuKάradiationwithdiffractionangle(2θ)rangefrom20^0to80^0andparticlesizeisdetermined by line broadening technique as shown below for all four samples. It is clear that, powder is partially amorphous and it is observed that calcined powders were of Perovskite structure and these were found to be similar with other XRD's of various authors. It is observed that, at higher temperatures, the noise in XRD is reduced. From the table 2 it is observed that as the concentration of Zr increased in B-Site of BSCF the density observed experimentally isnearly equal to the values calculated from theoretical values. The porosity values calculated for all the concentrations of Zr doped BSCF are nearly in the range of 97%. Hence, we can presume that the densification of materials is good and have the prominent role in the oxygen vacancies creation. It is also observed that the lattice constant for cubic Perovskite phase is nearly equal to all samples around the value a= 4.132915Å except in the Zr1sample with small increase of a=Å. From the XRD graph for BSCFZr, 1-4 samples it is observed the cubic phase structureand the Perovskite peak for 100% intensity at around**2θ** =31^0 with miller indices (110).

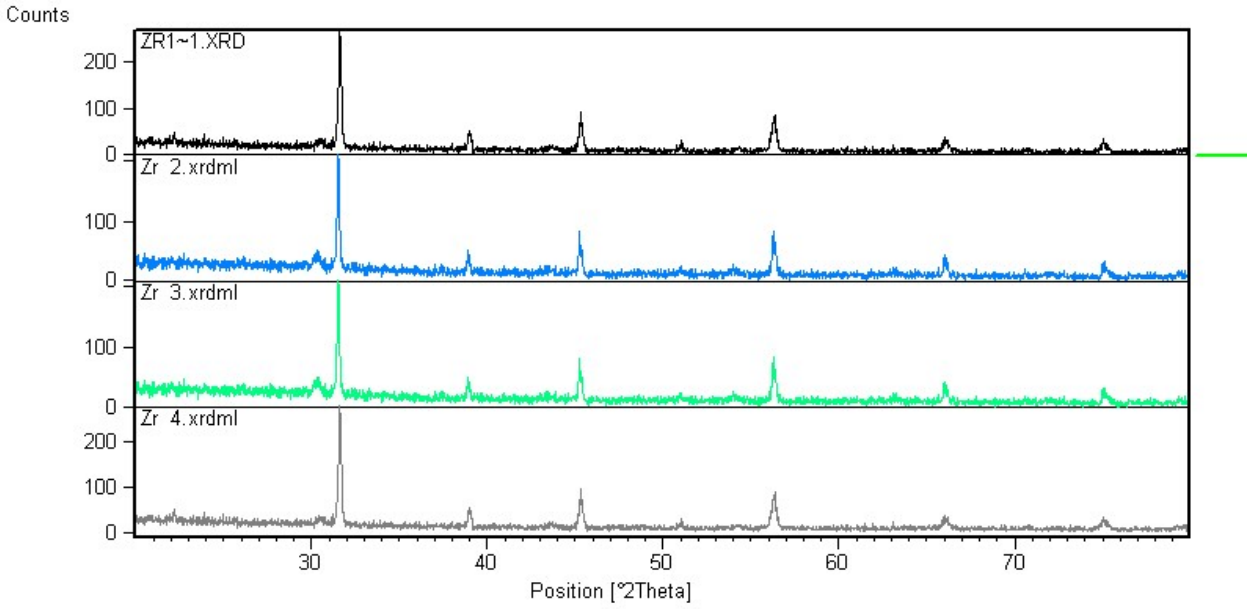


Figure.2X

RD Patterns of Ba0.5 Sr0.5 [Co0.8Fe0.2]1-xZrxO3-δ with δ=o, x=0, 0.1, 0.15, 0.20 calcined at 1050^0C.

Sample	2θ	θ	Cosθ	FWHM(β)	βCosθ	e size D=$\frac{0.9\lambda}{\beta\ COS\theta}$
Zr 1	31.5987	79935	222	723	0.4544565	0.30509
Zr 2	17.6511	2555	316	140	0.6067302	0.228526
Zr 3	18.2550	275	733	140	0.6062206	0.228718
Zr 4	19.1931	9655	50	093	0.4035698	0.343568

Table.3XRDdatafordeterminingtheaverageparticlesizeof BSCFZr (5582Zr)

From the Table.3, It is observed that the particle size of the samples $Zr_2$and $Zr_3$is nearly same around 0.228622nm, while for the sample$Zr_4$the particle size is around 0.324329nm is slightly greater than Zr_1 sample. That is pure BSCF sample.It is also observed that there is a variationin FWHM values.

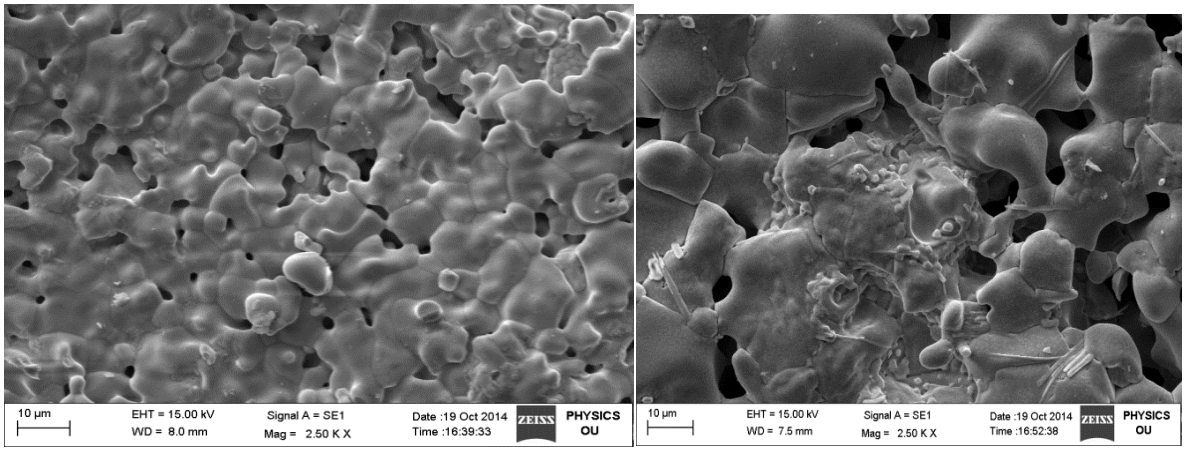
©IJRASET: All Rights are Reserved

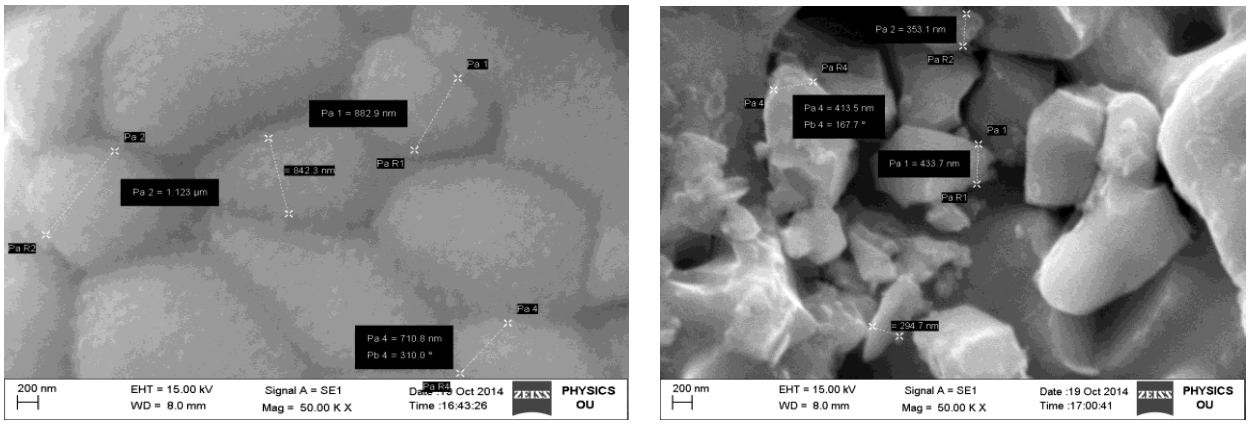
From the above data, the percentage density of the samples increased as partial substitution of lighter elements with heavier elementincreases due to the concentration of dopantZronB-site.Asaresult,theporosityofsamplesdecreasesbysmallamountdue todopantconcentration.Even ifporosity isoneofthe keycriteria forSOFC cathode materials,stabilityofmaterialalsoplaysagreatroleontheperformancesofSOFCs.The stabilitydependsonthecrystallineof material anditwasobserved hatthecrystalline natureofthesamplesincreasedastheconcentrationoffifthdopantonB-siteincreases. But theporosity of samples was not decreased that muchdue to the increment of dopant concentration.

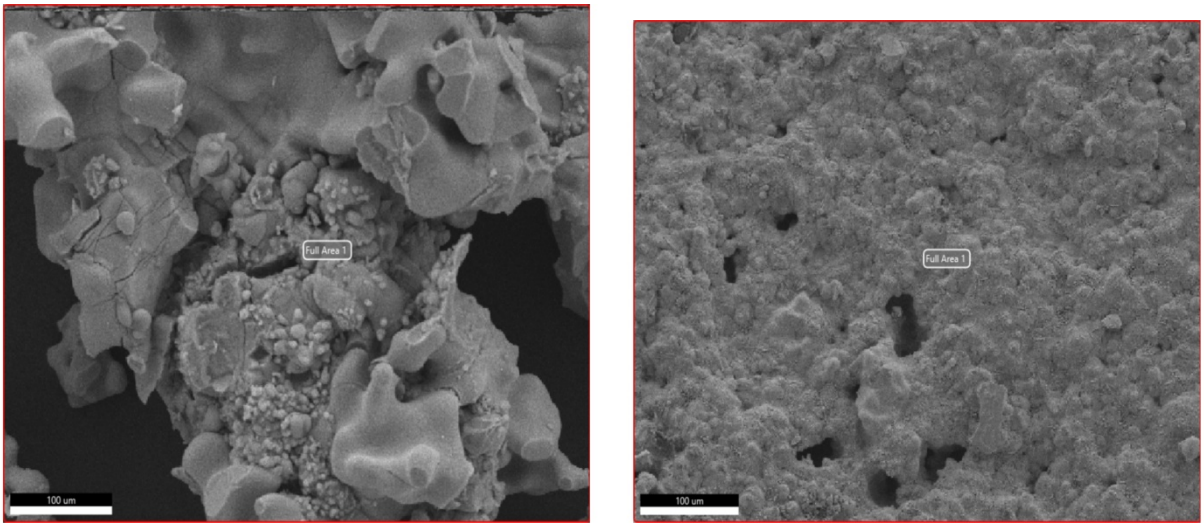
Therefore,dopingoffifthelementonB-sitehadgreatpositiveinfluenceon theperformanceoftheseSOFCcathodematerials. Thevariation ofparametersismore likelyacompensatoryresponseofthecrystalstructuretoaccommodatedopantsof different ionic size as compared to those of host ions which causes the shrinkageof crystal lattice that leads to decrease in the values of lattices constants and cell volume (V). The observedincreaseinthevalueofpercentagedensitywiththeincorporationofdopantions forallsynthesizedseriesisdueto(i) Largermolarmassofdopedmetalcationscompare to thatof host pair i.e. (CoFe)- Zrand (ii) shrinkage of latticethatleads to the observed decrease in thevalueof V.The results of average crystallite size of nano particles and lattice parameters are summarized observed.Asitisseenfromthe data, positionofthehighestintensity peakisdisplaceda smallamounttothehighangle duetotheconcentrationofdopantelementZr onB-site. Theplanegivingrisetothesmallest Braggangle wouldhavethehighestd-spacing. Averagecrystalline size, lattice parameterandcellvolumealsodecreaseswiththeincrement offifthdopantonB-siteduetotheshifting ofpositionanglewhichleadtothedecrement of d-spacing.As we have observedfrom theTable3, crystallinenature of theprepared materials increasedastheconcentrationoffifthdopantzirconiumincreases.Thisis provedbyseeingthevaluesof intensity peaks.Thevalueof intensity peaksincreasedmore as the concentration of fifth dopant Zr increased.

B. SCANNING ELECTRON MICROSCOPY (SEM)

Scanning electron microscopy (SEM) is applied to investigate the morphology of samples prepared in this work. By using a high resolution SEM, the structural properties of the synthesizedpelletswereanalyzedandrelatedthemwithphysicalbehaviorsoftheparticles asacathodematerial. Allsampleswereanalyzedbyhighresolution SEMmicrographsto know the densification of BSCFZ synthesized by sol-gel technique to be used themasintermediatetemperaturecathodematerials.Theobtained imagesfromSEM representthe variation inintensity ofthe signal collectedbythedetector asafunctionof X- Y space on the specimens. SEM Images are in fact two-dimensional representations of three- dimensional objects.However, the highdepth of field SEM lendsthree dimensionalappearances to the specimen images.Among the various interactions, secondary and backscattered electrons are generally utilized for micro structural investigations, sincetheir intensities varysensitivelywith surfacetopography,ahighresolutionSEM(ZEISS)was usedtoseethemorphology ofsynthesized samplesand torelate them with physicalbehaviors of the particlesused as a cathodematerial. In the present study SEM analysis was carried out by using the sintered pellets of the samples. SEM analysis is considered “non- destructive”,i.e., X-raysproduced byelectron interactionsdonot leadtoloss of sample volume, makingitpossible toanalyzethesame samplerepeatedly withoutaffectingthe prepared pellets.







Figures3a,3b,3c,3d,3e,3f

AsitisclearlyseenfromFigure,thecrystalconsistsofaperiodicarrangementof the unit cell into a lattice. The unit cell can contain a single or more atoms in a fixed arrangement. SEM micrograph clearly shows the presence of uniform grains with clean and distinct grain boundaries. It exhibited complete densification with a presence of pores on the surface.Grainboundaries are visible and the grain sizes are clearly increased.Theaverage grain size of the sample found from SEM image was 373.5nm. Increasing the sintering temperatureleadstocompletedensificationandposteriorgraingrowthandforce allmetals into the crystal network. The porosity has increased over the sample before debinding and sinteringbecause the loss of binding agentsused accountsfor the increased porosity. Decreasing of sample porosity is due to the increases of sintering temperatures used. This additionalsinteringhaspartiallycounteractedthepore-formingeffectofremovingthe bindingagents(Pike,2015). Figures**3a,3b,3c,3d,3e,3f** showsSEMmicrographofthe prepared sample for cathode material$\mathbf{Ba_{0.5}Sr_{0.5}(Co_{0.8}Fe_{0.2})_{1-x}Zr_xO_{3-\delta}(x=0.1)}$with high resolution at a magnification of 200nm.Using a high sintering temperature helps to transform the material from purely amorphous into a weakly crystalline structure. SEM micrograph clearly shows the presence of uniform grains with clean and distinct grain boundaries.Itexhibitedcompletedensificationwithapresenceofporesonthesurface. Grainboundaries are visible andthegrainsizes areclearlyincreased.Theaveragegrainsize ofthesamplefoundfromSEMimagewas373.5nm.Eventhoughthemicrostructure doesnotappeartobeaperfectPerovskitenetworkduetosomeimpuritiesinthesample,

wegotaperfectBSCFZPerovskitebyusingveryhighsinteringtemperaturebetween (900°C and1100°C).

Figures above shows a high resolution SEM micrographof the preparedsample for $\mathbf{Ba_{0.5}Sr_{0.5}(C\ o_{0.8}\ Fe_{0.2})_{1-x}Zr_xO_{3-\delta}(x=0.15)}$atamagnificationof200nm.

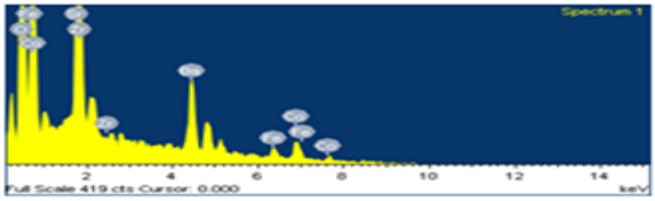
Asitcan be seen from the figure, particlesize was in nanometerrange which means thathigh temperatureandconcentrationsof Z r dopingleadstograingrowth.Itexhibitedcomplete densificationwithapresenceof poresonthesurface.Grainboundaries arevisibleandthe grainsizesareclearlyincreased.TheaveragegrainsizeofthesamplefoundfromSEM imagewas373. 5nm.Theaveragegrainsizeisdecreasedandshowsthesamplewas more stabilized.

Figures above shows a high resolution SEM micrograph of the prepared sample for **$Ba_{0.5}Sr_{0.5}(C o_{0.8} Fe_{0.2})_{1-x}Zr_xO_{3-\delta}$(x=0.2)**atamagnificationof200nm.Asitis visibleathighermagnifications, thecrystallinityseemstogetmoreestablishedrather than previous samples.Particle size was still in nanometer range.It exhibited complete densificationwithapresenceofporesonthe surface. Grain boundariesarevisibleand the grain sizes are clearly shown. As Thermo gravimetric results demonstrate higher temperaturesarenecessary forcompletedegradationofimpuritiesandthesinteringprocessathightemperatureleadstotheformationofasecondaryphaseatthesurface.Av erage grainsizes of thesamplefoundfromSEMimagewere 373. 5nm.Crystalsconsistof planesofatomsthatarespaceddistance'd 'apartwhichcan beresolvedintomany atomicplaneseachwithadifferent'd'spacinga,bandc (length).Theanglesbetween a, b and c (butfor cubic phase a=b=c) are lattice constantsor parameterswhich can be determinedby XRD termedas grain structures andtheregion where by each unitcell separatedweregrainboundary. When thesintering processtake placeduetothedifference in lattice parameters arrangement for the cubic phase of BSCFZr the holes are formed. In general, it is evidentthat the majority of synthesized samples are spherical with a uniform surface morphology.Thesurfacesof synthesizedsamplesexhibitwell defined crystalline nano particles. Few of them are formed as agglomerates of smaller particles and appeared as lumps. The grain growth of such agglomerates on the surface is however, normal.Theindividualnanoparticlesmaytendtocoalescencetogetherduetosinteringofthesamples at high temperatures of 950°C during synthesis. The average grain sizes in each of the synthesized series,getssmallerwhenthedopantcontentincreasesasalsoevidentfromXRDdata.Furtherreductioninaveragegrainsizesofparticlesfordo pedsamplesas comparedto undoped sample is owing to the incorporation of co-dopants in Perovskite cathodesanditisintherangeof -350nm.Inthisstudy,averagegrainsizeof allthe samples wascalculated bylinear intercept technique. The findings obtained are moreporousthan previousliteraturesthat werearound 5% (Sharma &Rao,2015).

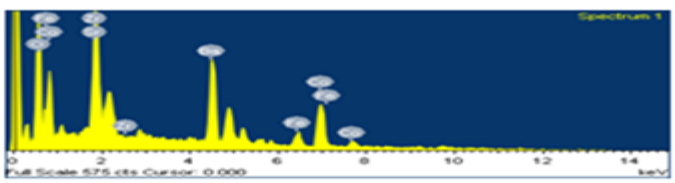
C. SEM with EDAX:

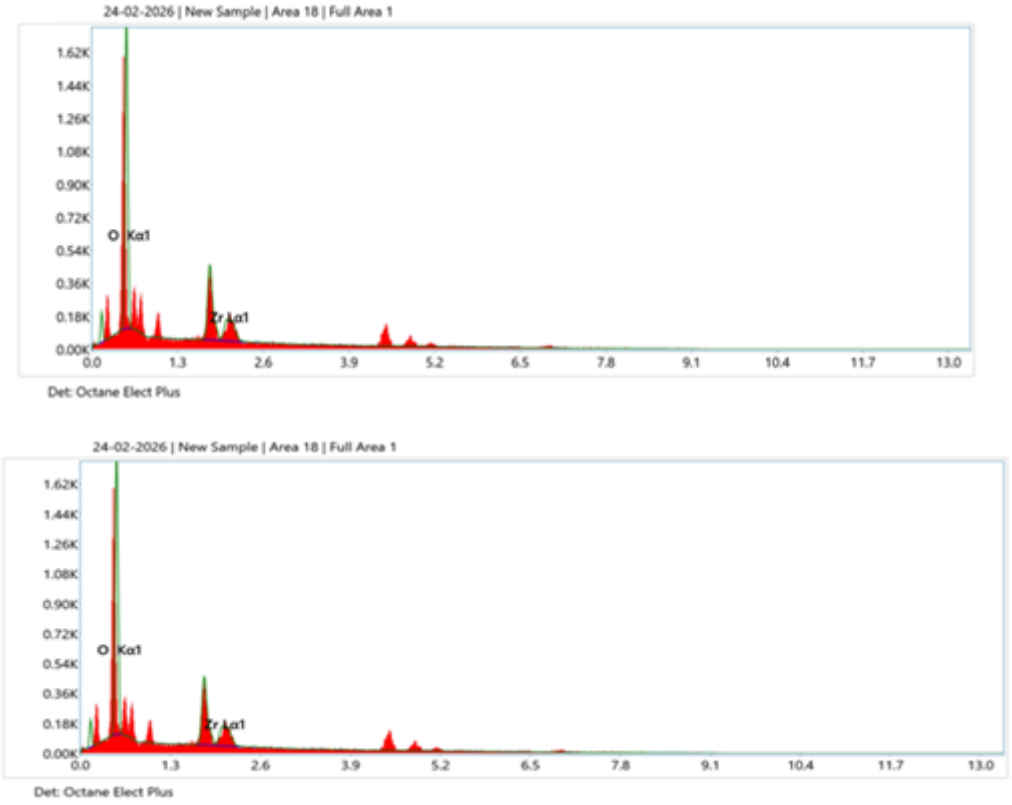
From SEM with EDAX analysis, it is found that the atomic percentage as taken in the formula is not changed and all atoms are present in the same proportion, particle sizesarenoted which areingoodcoincidencewiththedatataken from XRD. Thefigures4a,4b, 4c, 4d, 4e and 4f show the presence of Ba, Sr, Co, Fe, Zr peaks. The appearance of c may be due to usage of acetic acid. This C % has been reduced by calcining the samples at a higher temperature.Fromtheresultsofenergydispersivex-rayspectroscopy(EDS)analysis obtained, all thesampleshadtherequiredelementalcompositionwiththeirproportional weightandatomicpercentageasshowninFigureabove.Aswecanhave observedfrom Figureabovetheenergydispersivex-rayspectroscopy(EDS)graphsconfirmedthepresence of elements Ba, Sr, Co, Fe, Zr, O in the prepared samples and no other elements were observed.Elementalcompositions of some representative samples of each synthesized series withcompositionrevealedthattheelementalcompositionsofthesamplesarein conformitytotheirnominalstoichiometry asshowninTableabove.

Zr1



Zr2





Figures 4a, 4b, 4c, 4d

D. TGA/DTACHARACTERIZATION:

1) Introduction

Thermo gravimetric Analysis (TGA) and Differential Thermal Analysis (DTA) are used to study the thermal stability and decomposition behavior of materials. This report presents the analysis of two samples: Zr_1 and Zr_2.

The curves in figures 5(a) and 5(b) correspond to TGA (weight loss in % Vs temperature) and DTA (Rate of losing weight Vs temperature) for Ti1and Ti2samples.DTAis studied with difference in temperature and flow of heat between the sample and a reference. Moisture, Thermal stability and composition are studied simultaneously by TG/DTA referring Exothermic and Endothermic processes.

Powder samples of **Zr1** of 8.3mg and **Zr2** of 10.9mg are taken and corresponding curves are recorded. The weight loss is observed for three times in TGA first at 120^0C due to evaporation of moisture, second at400^0C due to evaporation of nitrates and third at 650^0C due to evaporation of other impurities because of usage of acids, bases etc.,.The melting point can be at about 1100^0C.TGA-DTAis performed to determine changes in weight in relation to change in temperature. Such analysis relies on a high degree of precision weight, temperature and temperatureschange.Allprecursorsamplesareplacedontheplatinumpanthatis suspendedfromtheanalyticalbalancelocatedoutsidethefurnacechamberof the instrumentTGAQ500V20.13Build39.Thebalanceiszeroedandthesamplecupis heatedupfromroomtemperatureto800°C.Powders of8.3mg,10.9mgweretakenandcorrespondingcurveswererecordedfor$\mathbf{Ba_{0.5}Sr_{0.5}(Co_{0.8}Fe_{0.2})_{(1-x)}Zr_xO_{3-\delta}}$atx=0,0.1,0.15& 0 . 2 respectively.TheTGAcurve calculationsofallsamplesonthis studyindicated that thedecomposition of calciteoccurred at lower temperature.The decompositions of nitrates affected by the amount of NO_2 gas presentduringfiring.As(Sharma&Rao,2015)stated,theweightloss isobservedthree timesinthecurve.Firstitwasduetoevaporation of moisture,seconddueto evaporationsofnitratesandthethirdduetoevaporationofotherimpuritiesthatcomes fromtheusageofacidsandbases.Allsamplesdisplayedaveryslightincreaseintherate of expansionabove800°C which maybe attributedtotheloss of oxygen leadingtothe reduction (and subsequentincreaseinradius)of theCo/Fe ontheBsite.However,this increaseinexpansionrateissmall,suggestinglimitedreductioninair.

ThecurvesinFigures5a,5brepresentsTGA(weightlossinpercentvs.temperature)andDTA(rateoflosingweightvstemperatures)for**$Ba_{0.5}Sr_{0.5}(Co_{0.8}Fe_{0.2})_{(1-x)}Zr_xO_{3-\delta}$** samplesatx=0,0.1, 0.15 and 0.2 respectively. As it is observed from Figures 5a,5b, there were weight losses observedthreetimesinthecurveforthepreparedsampleataconcentrationofx=0which isthereisnodopingoftitaniumonB-site.The firstweightlosswasaround1 2 0 °C dueto evaporationofmoisture,thesecondweightlosswasaround400°Cdueto evaporationof nitratesandthethirdweightlosswasaround650°Cduetoevaporationofotherimpuritiesthatcomesfromtheusageofacidsandbases.Thisresultt ellsinformationaboutthesinteringtemperaturesatwhichthepreparedsamplemustbe sintered. As we haveobservedfrom Figures 5(a),5(b), duetoevaporationof otherimpurities thatcomes from the usage of acids and bases. This result tells information about the sintering temperatures at which the prepared samplemust becalcinedandsintered.
duetoevaporationof moisture duetoevaporationofotherimpuritiesthatcomesfromtheusageofacidsandbases. Fromtheresultsobtained,informationaboutthesintering temperatures at which the preparedsamplemustbesinteredwastaken.Asitisseenfromthecurvesforallsamples,therewasamoreintensedegradationofnitratesatlowerte mperatures.Butmasslossisnotstabilizedperfectlyat8 0 0 °C.Thismightindicatethattherewereafewintermediatecompoundtobedecomp osed.Thistellsaninformationaboutthe sinteringtemperaturesmustbe largerthan8 0 0 °C todecompose allthecompoundsand remove theimpuritiesfrom samplescompletely.

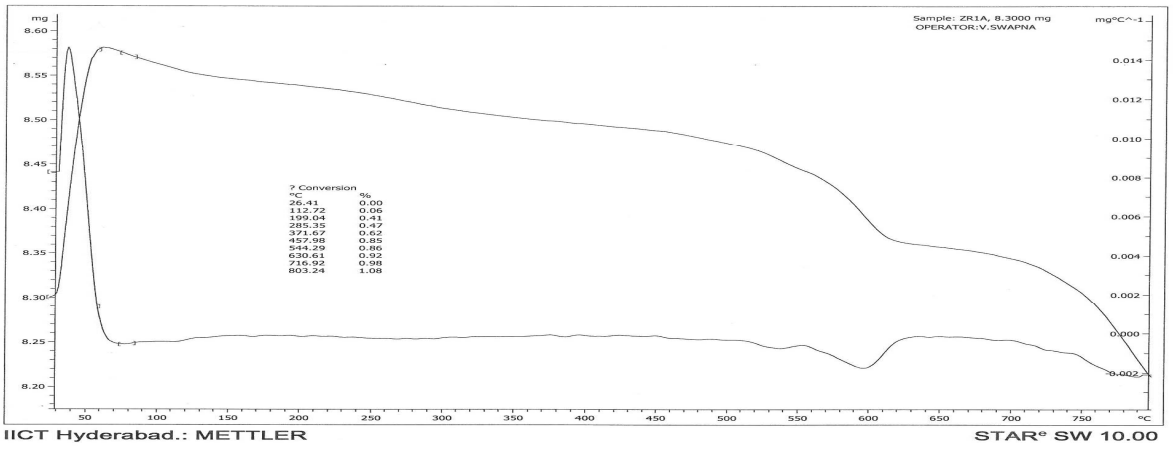


Figure 5(a) TGA/DTA Curves for$Ba_{0.5}Sr_{0.5}[Co_{0.8}Fe_{0.2}]_{0.9}Zr_{0.1}O_2$
Temperature (X-Axis), Weight loss in %(Y-Axis)

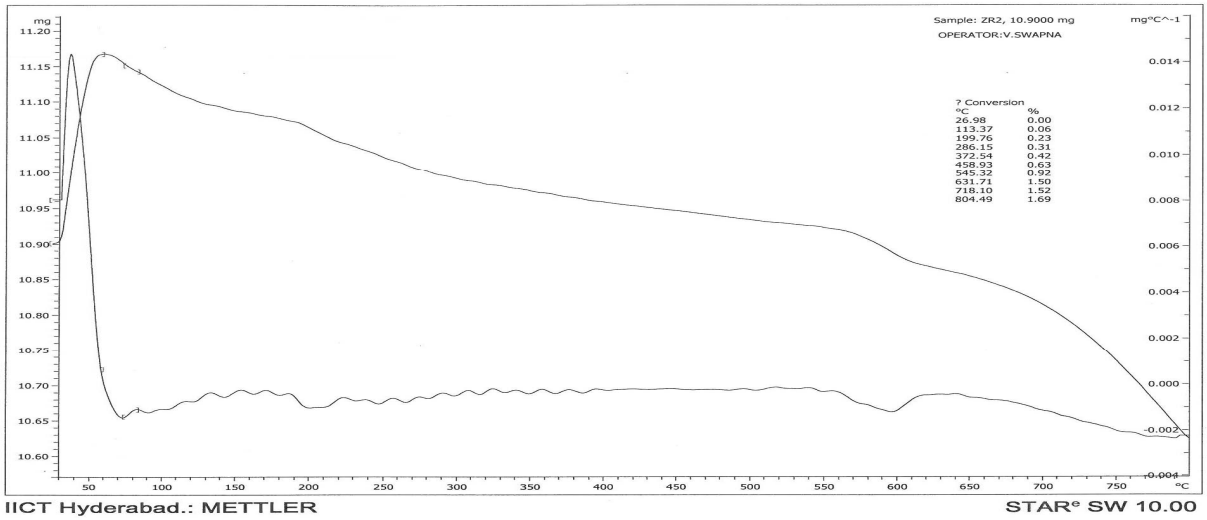


Figure 5(b) TGA/DTA Curves for $Ba_{0.5}Sr_{0.5}[Co_{0.8}Fe_{0.2}]_{0.85}Zr_{0.15}O_2$
Temperature (X-Axis), Weight loss in %(Y-Axis)

2) Sample Details

Sample	Initial Mass (mg)	Final Mass (mg)
Zr_1	8.30	8.20
Zr_2	10.90	10.63

Table(4)

3) Analysis of Sample Zr_1

Total Weight Loss: ~1.08%

Stages of Decomposition:

• 30–120°C: Moisture removal

• 120–400°C: Loss of volatile components

• 400–650°C: Structural changes

• 650–800°C: Final decomposition

DTA Observations:

• Small endothermic peak around 600°C

• No strong exothermic reactions.

4) Analysis of Sample Zr_2

Total Weight Loss: ~1.69%

Stages of Decomposition:

• 30–120°C: Moisture removal

• 120–400°C: Volatile loss

• 400–650°C: Pronounced decomposition

• 650–800°C: Final degradation

DTA Observations:

• Stronger endothermic peak near 600°C

• Minor fluctuations indicating structural changes.

5) Comparison of Zr_1 and Zr_2

Property	Zr_1	Zr_2
Total Weight Loss	~1.08%	~1.69%
Thermal Stability	Higher	Lower
DTA Peak Intensity	Mild	Stronger
High Temperature Behavior	Stable	More reactive

Table(5)

6) Conclusion

Both samples exhibit high thermal stability with minimal weight loss. Sample Zr_1 shows better stability compared to Zr_2. Zr_2 exhibits slightly higher decomposition and stronger thermal activity.

E. Fourier Transform Infrared (FTIR) spectroscopy:

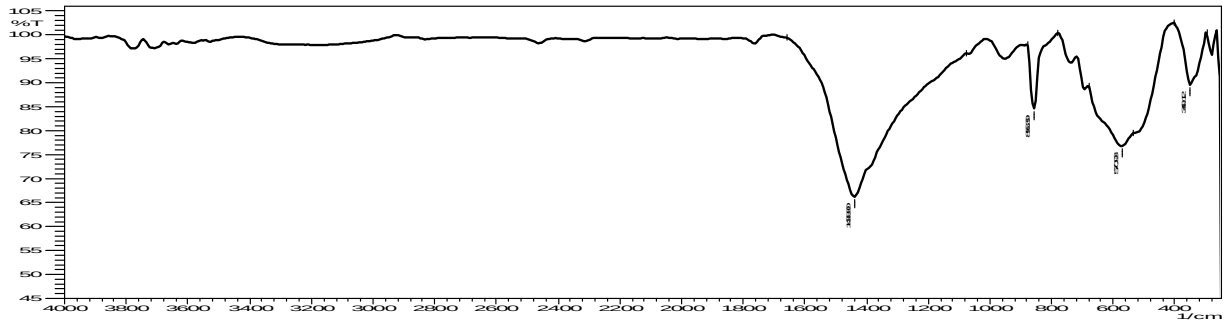


Figure.6 (a)

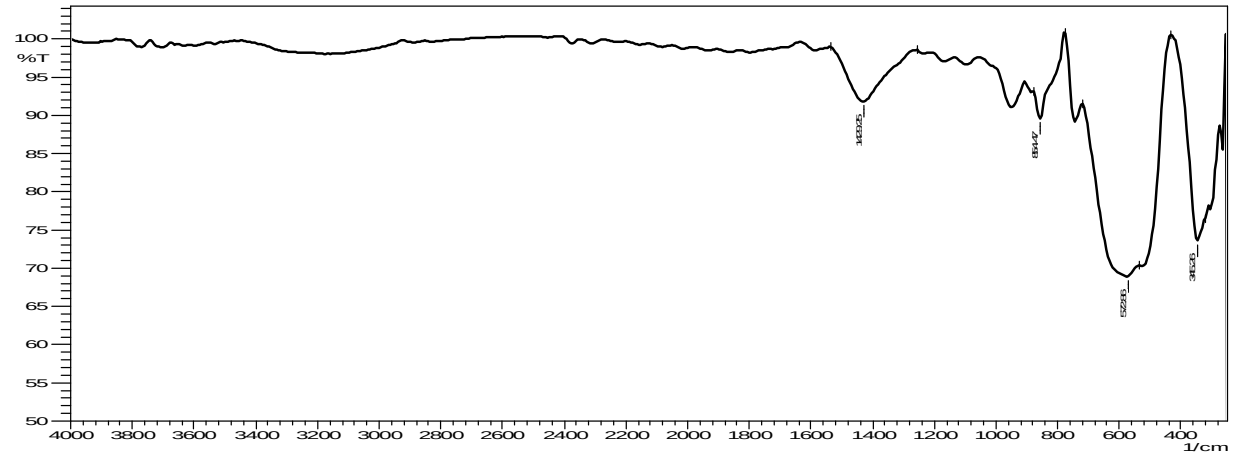


Figure.6 (b)

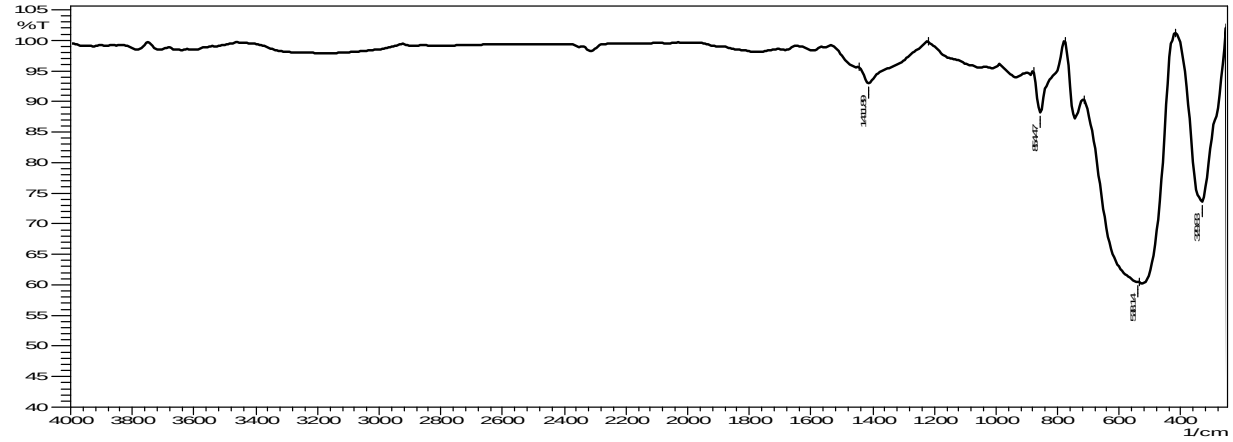


Figure.6 (c)

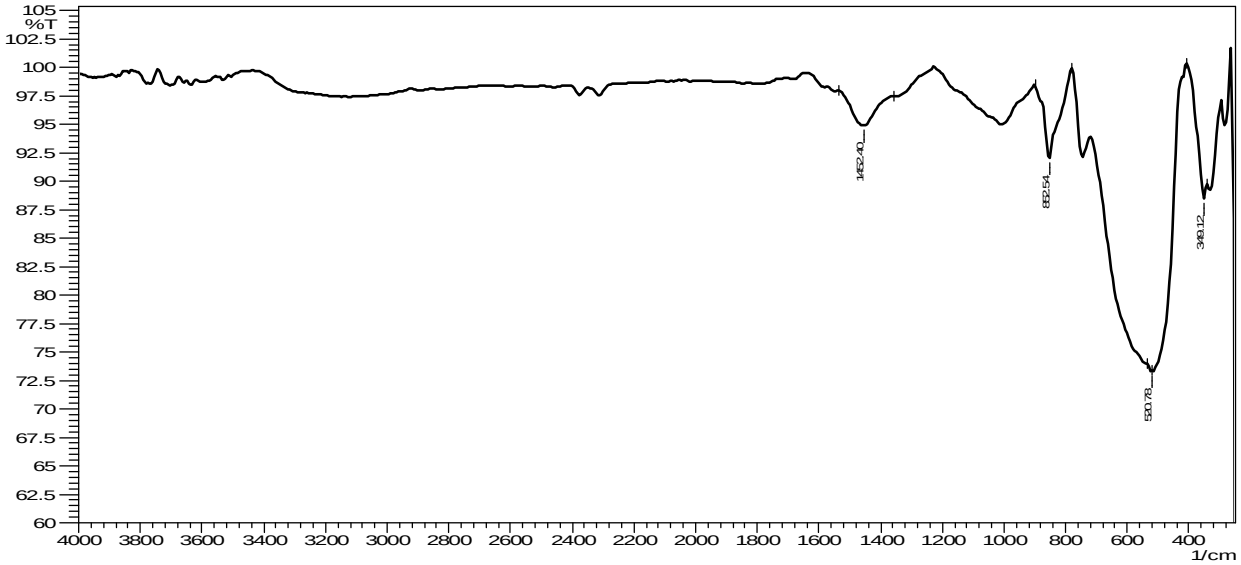


Figure.6 (d)

FTIR Analysis Report of Zirconium Oxide Samples

Four samples (Zr_1, Zr_2, Zr_3, and Zr_4) were analyzed using FTIR spectroscopy to study functional groups and bonding characteristics.

a) Common Observations

Broad peak ~3400–3200 cm^{-1} indicates O–H stretching (adsorbed water). Peaks ~1600–1400 cm^{-1} indicate H–O–H bending or carbonate traces. Strong peaks below 800 cm^{-1} correspond to Zr–O and Zr–O–Zr vibrations.

b) Sample-wise Analysis

Zr_1

- 1438 cm^{-1}: O–H bending
- 856 cm^{-1}: Zr–O
- 570 cm^{-1}: Zr–O–Zr
- 349 cm^{-1}: lattice vibration

Zr_2

- 1421 cm^{-1}: O–H bending
- 860 cm^{-1}: Zr–O
- 621 cm^{-1}: Zr–O–Zr
- 345 cm^{-1}: lattice vibration

Zr_3

- 1411 cm^{-1}: O–H bending
- 854 cm^{-1}: Zr–O
- 538 cm^{-1}: Zr–O–Zr
- 329 cm^{-1}: lattice vibration

Zr_4

- 1452 cm^{-1}: O–H bending
- 852 cm^{-1}: Zr–O
- 520 cm^{-1}: Zr–O–Zr
- 349 cm^{-1}: lattice vibration

S.No.	Sample	Hydroxyl Content	Crystallinity	Structural Order
1.	Zr_1	Lowest	Highest	Best
2.	Zr_2	High	Low	Moderate
3.	Zr_3	Moderate	Medium	Improved
4.	Zr_4	Lower	Higher	Good

Table 6 –Comparative table

Conclusion

All samples confirm zirconium oxide formation. From Zr_1 to Zr_4, hydroxyl content decreases while crystallinity and structural stability increase. Zr_1 shows the most well-defined oxide structure.

F. Impedance:

To characterize the electrochemical properties of BSCFZ cathode, AC impedance values are measured and characterization of cathode processes is based on the application of ac potential

$E(t) = E_oCos(\omega t + \phi)$ ---------- **(1)**

of minimum amplitude such that ac current $I(t) = I_oCos(\omega t - \phi)$ ---------- **(2)**

is obtained. Impedance, $Z=$ ---------- **(3)** is calculated at different AC frequencies up to few MHz.The impedance measurements characterizes the physical and chemical processes related to time constants ,electron transfer at high frequencies and mass transfer at low frequencies.

In the present study, the impedance measurements were carried from room temperature to 150^0 C and NY Quist plots ($Z_S = Z_{Real} + Z_{Imaginary}$) are drawn as shown in figures a& b
The cole-cole plots are observed for $\mathbf{Z^I}$ and $\mathbf{Z^{II}}$ plots are as depicted in figures a & b
AC conductivity is calculated by the formula = where Y^I is called admittance, t is thickness of the sample and A is area of the sample. The conductivities are tabulated in tables 2 & 3 below.

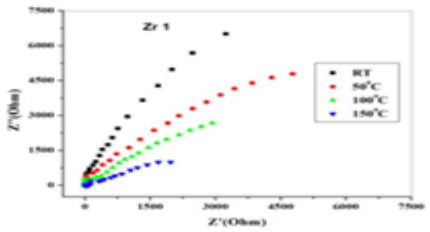


Fig. 7(a) Z^I Vs Z^{II} of Zr_1 Sample

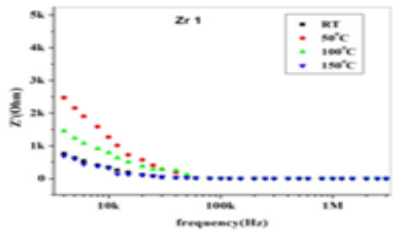


Fig 7(b)Frequency Vs Z^I of Zr_1 Sample

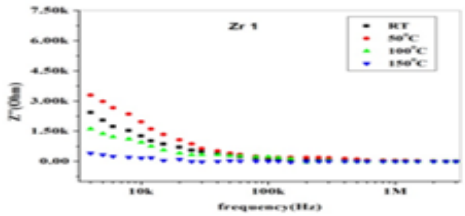


Fig. 7(c) Z^I Vs Z^{II} of Zr_1 Sample

Figure.7

S.No	Temperature	Resistance (ohm)	Admittance(Y)	Area(A)m^2	Thickness(t)m	$\sigma^I_{AC}=\frac{Y^I t}{A}$ S / m
1	Roomtemp.	1550	$4.925X10^{-4}$	$69.42X10^{-6}$	$1.46X10^{-3}$	$1.04x10^{-2}$
2	50	1125	$9.33X10^{-4}$	$69.42X10^{-6}$	$1.46X10^{-3}$	$1.96x10^{-2}$
3	100	486	$1.92\ X10^{-3}$	$69.42X10^{-6}$	$1.46X10^{-3}$	$4.04x10^{-2}$
4	150	198	$3.45\ X10^{-3}$	$69.42X10^{-6}$	$1.46X10^{-3}$	$7.26x10^{-2}$

Table6.Calculation of conductivities of Zr_1 Sample

S.No	Temperature	Resistance	Admittance	Area(A)m2	Thickness(t)m	$\sigma^I_{AC}=\frac{Y^I t}{A}$ S / m
1	Roomtemp.	380	$2.185X10^{-3}$	$70.6124X10^{-6}$	$1.42X10^{-3}$	$4.39x10^{-2}$
2	50	290	$4.186X10^{-3}$	$70.6124X10^{-6}$	$1.42X10^{-3}$	$8.42x10^{-2}$
3	100	105	0.01235	$70.6124X10^{-6}$	$1.42X10^{-3}$	$2.48x10^{-1}$
4	150	62	0.02	$70.6124X10^{-6}$	$1.42X10^{-3}$	$4.02x10^{-1}$

Table7.Calculation of conductivities of Zr2 Sample

From the tables, it is observed that as the temperature is increased the from rt to 150^0C the resistance of the all samples of BSCFZ1-4 decreased and subsequently conductivity increased in the order of ten times from 0.062 -0. 402.Further increase of temperature the resistance drops abnormal and electronic conductivity dominates, the ionicconductivity. In the contribution of total conductivity of samples. In general in perovskite samples most of them are ceramic nature the ionic conductivity contribute more at high temperature around 600^0C.Since BSCFZ samples contain metal ions, so electronic conductivity more rather than ionic conductivity, So to increase ceramic nature and improve ionic conductivity, the slight doping of Zr in the place of Fe, Co in the B- site of perovskite results the increase of ionicconductivity.

As the concentration of Zr slightly increased in BSCFZr the resistance is decreased and ac conductivity s increased as 0.084 to 0.402.s/m.

The Zr moderate doping in BSCFO cathodes will maintain phase stability (perovskite cubic) of the samples which observed in DTA-TGA experiment results the enhancement of diffusion pathways and results the increase of ionic conductivity in all samples. The major contribution for the conductivity is creation of oxygen vacancies which helps the oxygen ion migration from cathode to anode through electrolytes in SOFC.

Ionic conductivity in BSCF depends on oxygen vacancies (Vo'')which explained by koger-vink relations. Moderate doping of Zr can stabilize oxygen vacancies and maintain mixed ionic and electronic conductivity in BSCFZrsample Theactivation energies also for oxygen diffusion will maintain moderate and reach near to 1ev of oxygen ions.

IV. CONCLUSION

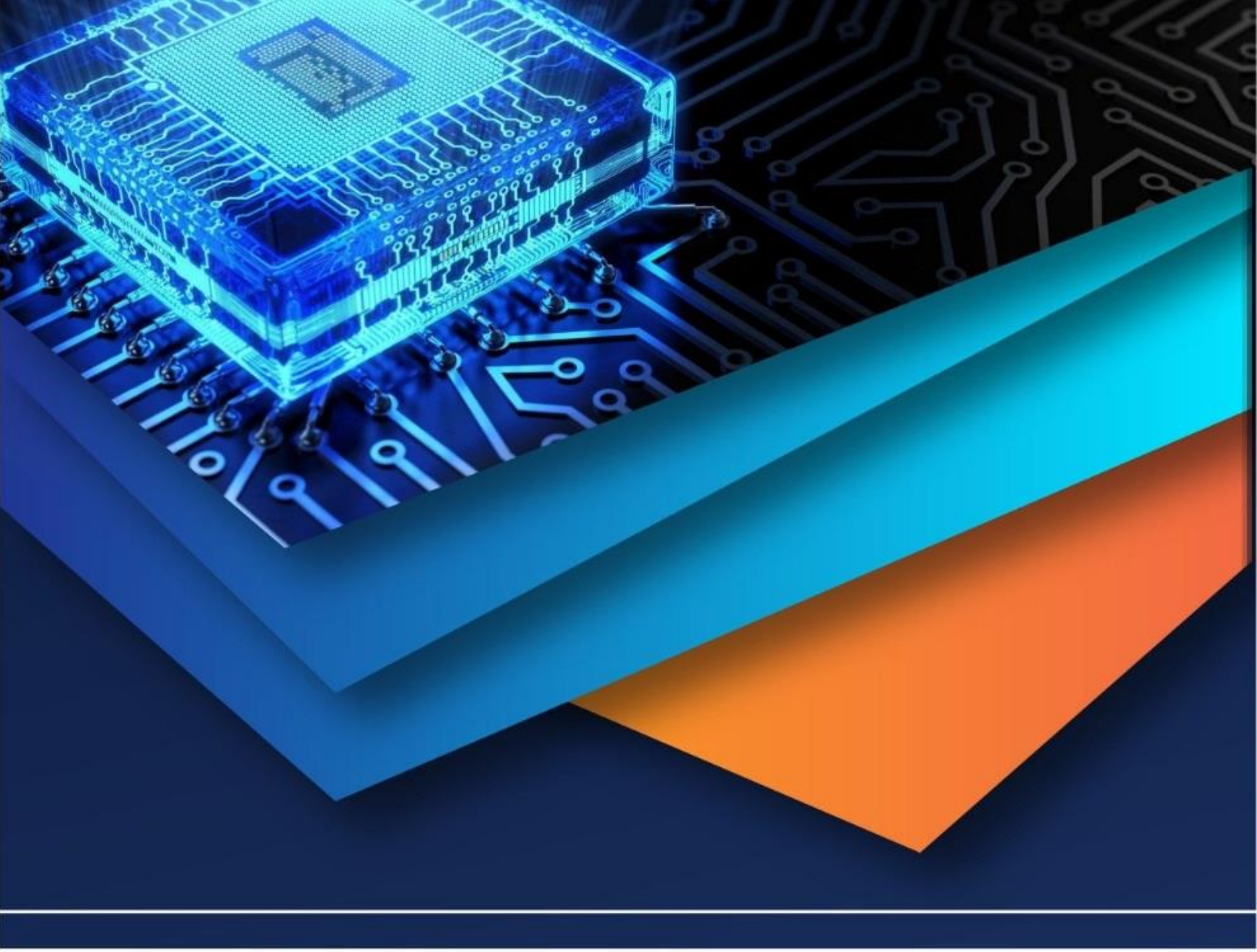
The moderate doping of Zr in BaSrCoFeO3 cathodes has improved the ionic conductivity at high temperatures by stabilizing the cubic perovskite structure indirectly by optimizing the oxygen vacancy distribution, enhancing oxygen diffusion pathways. It also reduced the Co/Fe redox activity can limitthe charge compensation and promising materials for mixed ionic electronic conductivity in cathodes of IT-SOFC**.**

REFERENCES

[1] T. Ishihara, H. Matsuda, Y. Takita, J. Am. Chem. Soc. 116(1994) 3801
[2] K. Huang, M. Feng, J.B. Goodenough, J. Electrochem. Soc.
[3] J.P.P. Hujismans, F.P.F. Berkel, G.M. Christie, J. Power
[4] R. Maric, S. Ohara, T. Fukui, H. Yoshida, M. Nishmura, T. Vol. PV 94-12, Electrochemistry Society, 1994, Inagaki, K. Miura, J. Electrochem. Soc. 146 2006
[5] P. Huang, A. Horks, A. Petric, J. Am. Ceram. Soc. 82 (1999) Electrochem. Soc. 134 (1978) 21412402
[6] F. Chen, M. Liu, J. Solid State Electrochem. 3 (1998) 7.Tuller (Eds) Proceeding 1st International Symposium Ionic
[7] T. Iśhihara, H. Matsuda, Y. Takita, in: Proceedings 2nd Ionic and Mixed Conducting Ceramics, Electrochemistry Soceity,and Mixed Conducting Ceramics, Vol PV 94-12, Electro- 1991, p. 122.Chemistry Soceity, 1994, p. 85.
[8] T. Ishihara, M. Honda, Y. Takita, Recent Res. Dev. Electrochem2 (1999) 15
[9] N.Q. Minh, T. Takahashi, in: Science and Technology ofNishiguchi, Y. Takita, J. Electrochem. Soc. 145 (1999) 3177. Ceramic Fuel Cell,1995, p. 147.
[10] S. Majumdar, T. Claar, B. Flandermeyer, J. Am. Ceram. Soc. 144 (1997) 3620. 69
[11] O. Yamamoto, Y. Takeda, R. Kanno, H.U. Anderson, SolidState Ionics 22 (1989)
[12] A. Hammouche, E. Siebert, A. Hammou, Mater. Res. Bull.24 (1989) 367.
[13] T. Ishihara, M. Honda, T. Shibayama, H. Minami, H. Nishiguchi, Y. Takita,
[14] J. A. Kilner, R.A. De Souza, I. C. Fullarton, Solid state IonicsP. SSC 86-88 (1996) 703. O2
[15] A Boudghene Stambouli and E, Traversa, Renewable and Suitable Energy Rev., 6.433 (2002)
[16] S. J. Skinner, Jnt. T. Inorganic Matter., 3, 113 (2001)
[17] Z. Shao and S. M. Haile, Nature (London) 431, 432, 170 (2004)
[18] Y. Itoh V, Nishida, A. Tomita, Y. Fujie. Solid state communication. 149. 41 (2008)
[19] B. Liu, Y. Zhamg and L. Tang, Int. J. Hydrogen Energy, 34, 435 (2009)
[20] X. Sun, S. Li, J. Sun, X. Liu, B. Zhu, Int. J. Electrochem. Sci. (2007) 462
[21] A. Subrahmania, T. Saradha, S. Muzumathi, J. Power Sources 165 (2007) 728
[22] H. Zhao, F. Mauvy, C. Lalanne, J.M. Bassat, S. Fourcade, J.C Grenier, Solid State Zonics 179 (2008) 2000
[23] A. Princivalle, E. D. Jurado, SSI 179 (2008) 1921
[24] V. B. Vert, J.M. Serra, Fuel Cells (2009) 663
[25] Y. Li, R. Gemmen, X. Liu, J. Power sources, 195 (2010) 3345[26] S.S. Shimizu, T. Yamaguchi, Y. fujishiro, ECS Tans. 25 (2009) 975
[26] Ionic transport modification in proton conducting BaCe0.6Zr0.3Y0.1O3−δwith transition Metal oxide dopants Solid State Ionics(2016) C. Jin
[27] EffectofBanonstoichiometryonthephasecomposition,microstructure,chemicalStabilityandelectricalconductivityofBaxCe0. 7Zr0.1Y0.1Yb0.1O3− δ(0.9≤x≤1.1)proton conductors. Ceram. Int.(2015)Y. Liu
[28] Enhanced sinter ability of BaZr0.1Ce0.7Y0.1Yb0.1O3−δby addition of nickel oxide J. Power Sources (2011) H.-I. Ji
[29] InfluenceofsinteringactivatorsonelectricalpropertyofBaZr0.85Y0.15O3-δproton- conducting electrolyte J. Power Sources (2021) L. Mahmud et al.
[30] Challenges in fabricating planar solid oxide fuel cells: a review Renew. Sustain. Energy Rev.(2017) U. Damo et al.
[31] Solidoxidefuelcellhybridsystem:adetailedreviewofanenvironmentallycleanand efficient source of energy (2019) D. Guo et al.
[32] Preparation and characterization of highly active and stable NdBaCo$_{0.8}$Fe$_{0.8}$Ni$_{0.4}$O$_5$+δ oxygenelectrode for solid oxide fuel cells Electrochim. Acta (2023) M. Jafari et al.
[33] Enhancement of an it-sofc cathode by introducing ysz: Electrical and electrochemical properties of la0. 6ca0. 4fe0. 8ni0. 2o3-δ-ysz composites Int. J. Hydrog. Energy (2019)C.W.Chenetal.
[34] Electrochemical performance of lanthanum calcium cobalt ferrite cathode interfaced to lamox electrolyte Solid State Ion.(2008)K. Efimov et al.
[35] Ca-containingco2-tolerantperovskitematerialsforoxygenseparationJ.Membr. Sci.(2012)M. Salehi et al.
[36] Oxygenpermeationandstabilitystudyof(la0.6ca0.4)0.98(co0.8fe0.2)o3-δmembranesJ. Membr. Sci. (2017)Z. Pan et al.

[37] Study of activation effect of anodic current on la0. 6sr0. 4co0. 2fe0. 8o3- δ air electrode in solid oxide electrolyzer cell Electrochim. Acta (2016) A.I. Klyndyuket al.
[38] Double substituted NdBa(Fe, Co, Cu)$_2$O$_5$+δ layered perovskites as cathode materials for intermediate-temperature solid oxide fuel cells–correlation between structure and electrochemical properties Electrochim. Acta (2022)A. Mroziński et al.
[39] Electrochemical properties of porous Sr0. 86ti0. 65fe0. 35o3 oxygen electrodes in solid oxide cells: Impedance study of symmetrical electrodes Int. J. Hydrog. Energy (2019)
[40] S. Dwivedi Solid oxide fuel cell: materials for anode, cathode and electrolytent. J. Hydrog. Energy(2020)P.Kaur.et.al
[41] Review of perovskite-structure related cathode materials for solid oxide fuel cellsCeram.Int. (2020)N. Mahato et al.
[42] Progress in materials science Progress in material selection for solid oxide fuel cell technology : A review Prog. Mater. Sci. (2015) M. Liang et al.
[43] Nickel-dopedBaCo0·4Fe0·4Zr0·1Y0·1O3-δasanewhigh-performancecathodeforbothoxygen-ion and proton conducting fuel cellsChem. Eng. J. (2021)Y. Yamaguchi et al.
[44] La0.65Ca0.35FeO3-δ as a novel Sr- and co-free cathode material for solid oxide fuel cells J. Power Sources (2020)L. Zhanget al.BaCo0·4Fe0·4Zr0·2O3-δ: evaluation as a cathode for ceria- based electrolyte IT-SOFCsJ. Alloys Compd. (2019)H.Y. Tu et al.
[45] Ln0.4Sr0.6Co0.8Fe0.2O3−δ (Ln=La, Pr, Nd, Sm, Gd) for the electrode in solid oxide fuel cellsSolid State Ionics (1999)C.-Y. Gu et al.
[46] High performance Ca-containing La2-xCaxNiO4+δ (0≤x≤0.75) cathode for proton-conducting solid oxide fuel cellsInt. J. Hydrog. Energy (2020)N.A. Baharuddin et al.
[47] Shortreviewoncobalt-freecathodesforsolidoxidefuelcellsInt.J.Hydrog.Energy(2017)
[48] J.Tongetal.
[49] Investigationofidealzirconium-dopedperovskite-typeceramicmembranematerialsfor oxygen separationJ. Membr. Sci. (2002)Z.P. Shao et al.
[50] Advancedsynthesisofmaterialsforintermediate-temperaturesolidoxidefuelcells Prog. Mater. Sci.(2012) K.S. Baek et al.
[51] Electrical conductivity characteristics of Sr substituted layered perovskite cathode (SmBa0.5Sr0.5Co2O5+δ) for intermediate temperature-operating solid oxide fuel cell Ceram. Int. (2022) A.I. Klyndyuket al.
[52] Structural and electrochemical characterization of YBa(Fe, Co, Cu)2O5+δ layered perovskites as cathode materials for solid oxide fuel cells Int. J. Hydrog. Energy (2021)S.L. Zhang et al.
[53] EffectofFedopingontheperformanceofsuspensionplasma-sprayedPrBa0.5Sr0.5Co2-xFexO5+δcathodesforintermediate-temperaturesolidoxidefuelcells Ceram.Int.(2017) S.Yooet al. 39)Investigation of layered Perovskite type NdBa1-xSrxCo2O5+δ(x=0, 0.25, 0.5, 0.75, and 1.0) cathodes for intermediate-temperature solid oxide fuel cells Electrochem.Acta (2013) A.Junet al.
[54] Optimization of Sr content in layered SmBa1-xSrxCo2O5+δ Perovskite cathodes for intermediate- temperature solid oxide fuel cells Int. J. Hydrog. Energy (2012) S. Choi et al.
[55] Electrochemical properties of an ordered Perovskite LaBaCo2O5+δ-Ce0.9Gd0.1O2-δ composite cathode with strontium doping for intermediate-temperature solid oxide fuel cells Electrochem. Commun. (2013) H.P. Ding et al.
[56] PrBa0.5Sr0.5Co2O5+δlayeredperovskitecathodeforintermediatetemperaturesolidoxidefuelcells Electrochim. Acta (2010)F. Zhao et al.
[57] Layered perovskite PrBa0.5Sr0.5Co2O5+δ as high performance cathode for solid oxide fuel cells using oxide proton-conducting electrolyte J. Power Sources (2010) F.J. Jin et al.
[58] Characterization and evaluation of double Perovskite LnBaCoFeO5+δ(ln=Pr and Nd) as intermediate-temperature solid oxide fuel cell cathodes J. Power Sources (2013)

.



10.22214/IJRASET

45.98

IMPACT FACTOR: 7.129

IMPACT FACTOR: 7.429

INTERNATIONAL JOURNAL FOR RESEARCH

IN APPLIED SCIENCE & ENGINEERING TECHNOLOGY

Call : 08813907089 (24*7 Support on Whatsapp)